

Recruitment prediction for multi-centre clinical trials based on a hierarchical Poisson-gamma model: asymptotic analysis and improved intervals

Rachael Mountain¹ and Chris Sherlock¹

¹Department of Mathematics and Statistics, Lancaster University, UK.

Abstract

We analyse predictions of future recruitment to a multi-centre clinical trial based on a maximum-likelihood fitting of a commonly used hierarchical Poisson-Gamma model for recruitments at individual centres by a particular census time. We consider the asymptotic accuracy of quantile predictions in the limit as the number of recruitment centres, C , grows large and find that, in an important sense, the accuracy of the quantiles does not improve as the number of centres increases. When predicting the number of further recruits in an additional time period, the accuracy degrades as the ratio of the additional time to the census time increases, whereas when predicting the amount of additional time to recruit a further n^+ patients, the accuracy degrades as the ratio of n^+ to the number recruited up to the census period increases. Our analysis suggests an improved quantile predictor. Simulation studies verify that the predicted pattern holds for typical recruitment scenarios in clinical trials and verify the much improved coverage properties of prediction intervals obtained from our quantile predictor. Further studies show substantial improvement even outside the range of scenarios for which our results strictly hold.

Keywords: Clinical trial recruitment; recruitment prediction interval; multi-centre clinical trial; Poisson process; asymptotic analysis; asymptotic correction.

1 Introduction

Randomised controlled trials represent the gold standard for evaluating the safety and efficacy of a new healthcare intervention or treatment [1]. Such trials can require thousands

of patients, and so will typically recruit from tens or hundreds of centres. The timely recruitment of patients is widely recognised as a key determinant of the success of a clinical trial [2]. Nonetheless, sources suggest as many as 86% of all clinical trials fail to reach their required recruitment goals [3][4][5]. Failure to meet recruitment targets can have numerous negative implications, yet arguably the most critical is inadequate statistical power. In such a scenario, there is an increased risk of type II error, thus potentially preventing or delaying an effective treatment from being approved [6].

Future recruitment is often predicted using deterministic methods, based on the number already recruited up to that time, or historical data [7]. Such an approach is inadequate due to the stochastic nature of the recruitment process, and a number of stochastic models have been proposed.

Senn [8] considers a Poisson-based model for a multicentre clinical trial where recruitment follows a Poisson process with a fixed study-wide rate, $\lambda \geq 0$. The time to recruit a given number of patients then follows a gamma distribution. The underlying assumption that recruitment follows a Poisson process is well-accepted in the literature, with many articles exploring the inhomogeneous model, with a time-dependent rate [2][7][9][10].

The basic Poisson model outlined above fails to incorporate variation in recruitment rate across centres, as well as the uncertainty in the rate estimate. Anisimov and Fedorov [11] propose a random effects model in which recruitment follows a homogeneous Poisson process within each centre, with the centre-specific rates viewed as a sample from a gamma distribution. The time to recruit a given number of patients then follows a Pearson type VI distribution, while the number recruited in a given time is negative binomial. This model accounts for staggered centre initiation times and provides a method for predicting recruitment for new centres entering the trial. Citations of [11] on Google Scholar show that it has also been used by major pharmaceutical companies and in statistical software to plan drug production and distribution across centres during clinical trials. Further details of the model will be given in Section 2.

The Anisimov and Fedorov model (henceforth AF) has been developed and extended in numerous directions. For example, Bakshi et al. [12] suggest an extra level of hierarchy to incorporate variation from trial to trial in the gamma distribution parameters, with an aim to forecast recruitment for trials yet to begin. Mijoule et. al [13] propose a Pareto mixture distribution for the centre rates in place of the gamma. Further, [10] and [14] both incorporate time-varying rates into the AF model, with the latter also incorporating parameter uncertainty using the Bayesian paradigm.

Alternative methods have been suggested for modelling patient recruitment outside the Poisson approach, including Monte Carlo simulation [15], time series analysis [16], Brownian motions [17][18], and a nonparametric approach [19].

We investigate future predictions based on a maximum likelihood fit of the AF model to multi-centre recruitment data, where a total of N_\bullet patients has been recruited over C centres by a census time, t . We then consider two scenarios where prediction intervals are required, either for (1) the total number N_\bullet^+ recruited over some additional time t^+ , or (2) the total time T^+ to obtain n_\bullet^+ additional recruits. In this section, for brevity, we focus on scenario (1); similar methods and results are obtained for scenario (2).

Within the AF model, the distribution of the predicted number of recruits, \tilde{N}_\bullet^+ , has a negative binomial distribution, which depends on the observed data via the maximum likelihood estimates of the model parameters (MLEs); in contrast, the true number recruited, $N_\bullet^+ \sim \text{Poisson}(\lambda_\bullet t^+)$, where λ_\bullet is the sum of the recruitment rates of the individual centres. Let \hat{q}_p be the p th quantile of \tilde{N}_\bullet^+ ; *i.e.*, the predicted quantile. We first investigate $P_p := \mathbb{P}(N_\bullet^+ \leq \hat{q}_p)$ in the limit as $C \rightarrow \infty$, and empirically for finite C , and show that the key determinant of the behaviour is the ratio t^+/t . The desirable result of $P_p = p$ is only recovered in the limit as $t^+/t \rightarrow 0$, whereas in more typical scenarios P_p can be very different from p . The underlying reason for this is that the uncertainty in the MLEs is not being accounted for. Our asymptotic approximation to P_p feeds in to a new methodology which allows us to produce tractable prediction intervals, which have a coverage that is very close to that intended, and with a fraction of the computational cost of any bootstrap-based scheme.

Our theory, and hence our adjusted interval, is derived under the assumption that all centres opened at the same time; however, sometimes this is not the case. For example, given a predicted shortfall, perhaps based on our theory, it may be decided to open a new set of centres as well as keeping the existing centres going. Alternatively, or in addition, the existing centres may have been opened at different times. Guided by our theory, we provide an intuitive, tractable methodology for creating a prediction interval in such cases and demonstrate its accuracy in practice via extensive simulation studies.

Section 2 describes the AF model in detail, and Section 3.1 provides the asymptotic analysis in the case where all centres opened at the same time and details the methodology for creating prediction intervals with almost perfect coverage. Section 3.2 describes an empirical extension to this methodology for situations where the centres opened at different times. Our results and methods are verified via a detailed simulation study in Section 4, and our main result, Theorem 1 is proved in Section 5. First, however, we define the notations that will be used throughout.

1.1 Notations

Let C be the number of centres, and for $c = 1, \dots, C$, let t_c and N_c represent the time for which centre c was open before the census time and number recruited in centre c during the time t_c . The shorthand \underline{N} refers to the vector (N_1, \dots, N_C) , we let $N_\bullet := \sum_{c=1}^C N_c$, and

when all centres are open for the same time we denote that time by t . For Scenario One, let t^+ be the additional time ahead at which predictions will be made, and let N_c^+ be the number recruited in centre c in that time, with $N_\bullet^+ = \sum_{c=1}^C N_c^+$. For Scenario Two, let n^+ be the additional number of recruits sought and let T^+ be the additional time taken to recruit this number. The negative binomial distribution of the number of successes until there are a failures when the probability of success is p is denoted $\mathbf{NB}(a, p)$.

We use the notation \xrightarrow{p} and \Rightarrow to indicate convergence in probability and in distribution, respectively, and Φ to indicate the cumulative distribution function of a $\mathbf{N}(0, 1)$ random variable.

2 Model and prediction set up

2.1 Model, data and likelihood

The model assumes that the recruitment rate at centre c , for $c = 1, \dots, C$, is λ_c , where each λ_c is drawn independently from

$$\lambda_c \sim \mathbf{Gam}(\alpha, \beta). \quad (1)$$

Data for centre c are $n_c^1, \dots, n_c^{t_c}$, $n_c := \sum_{s=1}^{t_c} n_c^s$ and $n_\bullet = \sum_{c=1}^C n_c$. The likelihood for centre c is

$$\begin{aligned} L(\alpha, \beta, \theta; n_c^{1:t_c}) &= \int_0^\infty \frac{\beta^\alpha}{\Gamma(\alpha)} \lambda^{\alpha-1} \exp(-\beta\lambda) \prod_{s=1}^{t_c} \frac{\lambda^{n_c^s}}{n_c^s!} \exp(-\lambda) d\lambda \\ &\propto \frac{\beta^\alpha}{\Gamma(\alpha)} \int_0^\infty \lambda^{\alpha+n_c-1} \exp[-\lambda(\beta + t_c)] d\lambda \\ &= \frac{\Gamma(\alpha + n_c)}{\Gamma(\alpha)} \frac{\beta^\alpha}{(\beta + t_c)^{\alpha+n_c}}. \end{aligned}$$

Hence, up to an additive constant, the log-likelihood given data n_c^s , $s = 1, \dots, t$, $c = 1, \dots, C$, is

$$\ell(\alpha, \beta) = C\alpha \log \beta - \sum_{c=1}^C (\alpha + n_c) \log(\beta + t_c) - C \log \Gamma(\alpha) + \sum_{c=1}^C \log \Gamma(\alpha + n_c). \quad (2)$$

Thus $\underline{n} = (n_1, \dots, n_C)$ is a sufficient statistic. In the special case where $t_1 = \dots = t_C = t$, the second term in (2) reduces to $-(C\alpha + n_\bullet) \log(\beta + t)$ and, as we shall see in Lemma 1, $\hat{\alpha}/\hat{\beta}$ depends on \underline{n} only through n_\bullet .

2.2 Prediction

Since $N_c | \lambda_c \sim \text{Po}(\lambda_c t_c)$, given a prior of $\text{Gam}(\hat{\alpha}, \hat{\beta})$ for λ_c and an observation of n_c , the posterior distribution for λ_c is $\text{Gam}(\hat{\alpha} + n_c, \hat{\beta} + t_c)$. The distribution of $\lambda_{\bullet} := \sum_{c=1}^C \lambda_c$ is not tractable in general, but in the special case where $t_1 = \dots = t_C = t$, $\lambda_{\bullet} \sim \text{Gam}(C\hat{\alpha} + n_{\bullet}, \hat{\beta} + t)$. In this case, since $N_{\bullet}^+ | \lambda_{\bullet} \sim \text{Po}(\lambda_{\bullet} t^+)$, marginalising over λ_{\bullet} , the predicted total recruitment in further time t^+ is

$$\tilde{N}_{\bullet}^+ \sim \text{NB} \left(C\hat{\alpha} + n_{\bullet}, \frac{t^+}{\hat{\beta} + t + t^+} \right), \quad (3)$$

which has moments of

$$\mathbb{E} [\tilde{N}_{\bullet}^+] = \frac{C\hat{\alpha} + N}{\hat{\beta} + t} \times t^+ \quad \text{and} \quad \text{Var} [\tilde{N}_{\bullet}^+] = \frac{C\hat{\alpha} + N}{\hat{\beta} + t} \times t^+ \times \frac{\hat{\beta} + t + t^+}{\hat{\beta} + t}. \quad (4)$$

Alternatively, if the number of additional recruits is fixed at n^+ then, $T^+ | \lambda_{\bullet} \sim \text{Gam}(n^+, \lambda_{\bullet})$, so in the case where $t_1 = \dots = t_C = t$, the predicted further time \tilde{T}^+ to recruit these has a Pearson VI distribution [20] with a density of

$$f(\tilde{t}^+) = \frac{\Gamma(C\hat{\alpha} + n + n^+)}{\Gamma(C\hat{\alpha} + n)\Gamma(n^+)} \frac{\hat{\beta}^{C\hat{\alpha} + n} (\tilde{t}^+)^{n^+ - 1}}{(\hat{\beta} + t + \tilde{t}^+)^{C\hat{\alpha} + n + n^+}}. \quad (5)$$

Thus \tilde{T}^+ has moments of:

$$\mathbb{E} [\tilde{T}^+] = \frac{(\hat{\beta} + t)n^+}{C\hat{\alpha} + N - 1} \quad \text{and} \quad \text{Var} [\tilde{T}^+] = \mathbb{E} [\tilde{T}^+] \times \frac{(\hat{\beta} + t)(C\alpha + N + n^+ - 1)}{(C\alpha + N - 1)(C\alpha + N - 2)}. \quad (6)$$

3 Asymptotic analysis and methodology

We consider the properties of the quantile estimates under repeated sampling, so that \underline{N} is a random variable, and $\hat{\alpha}$ and $\hat{\beta}$ are, therefore, random. We examine the probability under the true data-generating mechanism that the quantity of interest, N_{\bullet}^+ or T^+ , will be less than its predicted quantile. This then leads to a tractable formula for an alternative probability, $p^*(p)$, such that $\mathbb{P}(N_{\bullet}^+ \leq \hat{q}_{p^*}) \approx p$ or $\mathbb{P}(T^+ \leq \hat{q}_{p^*}) \approx p$, and hence to prediction intervals with close to the intended coverage. In Section 3.1 we consider the scenario where all centres have been open for the same time; an intuitive extension for the more general scenario is given in Section 3.2.

3.1 All centres opened simultaneously

When all centres have been open for the same time, t , $N_{\bullet} \sim \text{Po}(\lambda_{\bullet} t)$ is the key (random) summary of the data, instead of n_{\bullet} for the specific realisation; thus $\hat{\alpha}$ and $\hat{\beta}$ are random. Importantly, in this case $\hat{\alpha}/\hat{\beta}$ depends on \underline{N} only through N_{\bullet} .

Lemma 1. When $t_1 = \dots = t_C = t$, the MLE for the likelihood in (2) satisfies $\widehat{\alpha}/\widehat{\beta} = N_{\bullet}/(Ct)$.

Proof. Set $\gamma = \alpha/\beta$; from the invariance principle it is sufficient to show that $\widehat{\gamma} = N_{\bullet}/(Ct)$. Substituting for β and ignoring terms only in α , (2) becomes:

$$\begin{aligned}\ell(\alpha, \gamma) &= -C\alpha \log \gamma - (C\alpha + N_{\bullet}) \log(\alpha/\gamma + t) \\ &= N_{\bullet} \log \gamma - (C\alpha + N_{\bullet}) \log(\alpha + \gamma t).\end{aligned}$$

Thus

$$\partial_{\gamma} \ell = \frac{N_{\bullet}}{\gamma} - \frac{C\alpha + N_{\bullet}}{\alpha + \gamma t} \times t = \frac{\alpha}{\gamma(\alpha + \gamma t)} (N_{\bullet} - \gamma Ct),$$

which is zero (and a maximum for ℓ) when $\gamma = N_{\bullet}/(Ct)$, as required. \square

We now state our main result, in which Z represents the limiting distribution of $(N_{\bullet} - \lambda_{\bullet}t)/\sqrt{\lambda_{\bullet}t}$. Strictly, Theorem 1 refers to a countably infinite sequence of centres, and observations, with $N_{\bullet}^{(C)} := \sum_{c=1}^C N_c$ and $\lambda_{\bullet}^{(C)} := \sum_{c=1}^C \lambda_c$, for $C = 1, \dots, \infty$. Likewise, N_{\bullet}^+ , T^+ , $\widehat{\alpha}$, $\widehat{\beta}$ and \widehat{q}_p (but not t^+ nor a) are implicitly indexed by C . For simplicity of presentation we suppress these superscripts.

Theorem 1. Let $\widehat{\alpha}$ and $\widehat{\beta}$ be the (random) maximum likelihood estimates from data N_1, \dots, N_C using the negative-binomial likelihood in (2), and let $Z \sim N(0, 1)$.

1. If \widehat{q}_p is the estimate from (3) of the p th quantile of N_{\bullet}^+ , the number recruited after a further time t^+ , then as $C \rightarrow \infty$ with t and t^+ fixed,

$$\lim_{C \rightarrow \infty} \mathbb{P}(N_{\bullet}^+ \leq \widehat{q}_p \mid \underline{N}) \stackrel{D}{=} \Phi \left(\sqrt{\frac{t^+}{t}} Z + \Phi^{-1}(p) \sqrt{1 + \frac{t^+/\beta}{1 + t/\beta}} \right).$$

However, if q_p is the true quantile of N_{\bullet}^+ , then for large C , $\widehat{q}_p/q_p - 1 = \mathcal{O}(1/\sqrt{C})$. If, in addition, t^+ is small, then $\widehat{q}_p/q_p - 1 = \mathcal{O}(\sqrt{t^+}/(Ct))$.

2. If \widehat{q}_p is the estimate from (5) of the p th quantile of T^+ , the time until n^+ further patients have been recruited, then as $C \rightarrow \infty$ with t fixed and n_{\bullet}^+ a function of C such that $n_{\bullet}^+/C \rightarrow a > 0$,

$$\lim_{C \rightarrow \infty} \mathbb{P}(T^+ \leq \widehat{q}_p \mid \underline{N}) \stackrel{D}{=} \Phi \left(-\sqrt{\frac{a\beta}{\alpha t}} Z + \Phi^{-1}(p) \sqrt{1 + \frac{a/\alpha}{1 + t/\beta}} \right).$$

However, if q_p is the true quantile of T^+ , then $\widehat{q}_p/q_p - 1 = \mathcal{O}(1/\sqrt{C})$. If, in addition, a is small, then $\widehat{q}_p/q_p - 1 = \mathcal{O}(a/\sqrt{C})$.

Theorem 1 is proved in Section 5. We discuss the consequences for N_{\bullet}^+ in detail; those for T^+ are analogous.

For the median, Theorem 1 suggests that $\mathbb{P}(N_{\bullet}^+ \leq \hat{q}_{0.5}) \approx \Phi(\sqrt{t^+/t}Z)$, so that when $t^+ \approx t$, this probability is approximately uniformly distributed on $[0, 1]$. By contrast, when $t^+ \ll t$ the probability concentrates at ≈ 0.5 as is desirable, and when $t^+ \gg t$ the probability concentrates around 0 and 1 each with a mass of 0.5, which is not desirable. The theoretical densities for $\mathbb{P}(N_{\bullet}^+ \leq \hat{q}_{0.5})$ as a function of t (with $t^+ = 400 - t$) are given in Figure 1. For more general quantiles, with t fixed, as $t^+ \rightarrow 0$, the probability approaches a point mass at p as desired, but as $t^+ \rightarrow \infty$ the same concentration around 0 and 1 happens, however, the mass on 1 is $\mathbb{P}\left(Z \geq -\sqrt{t/(\beta+t)}\Phi^{-1}(p)\right) = \Phi(\sqrt{t/(\beta+t)}\Phi^{-1}(p))$.

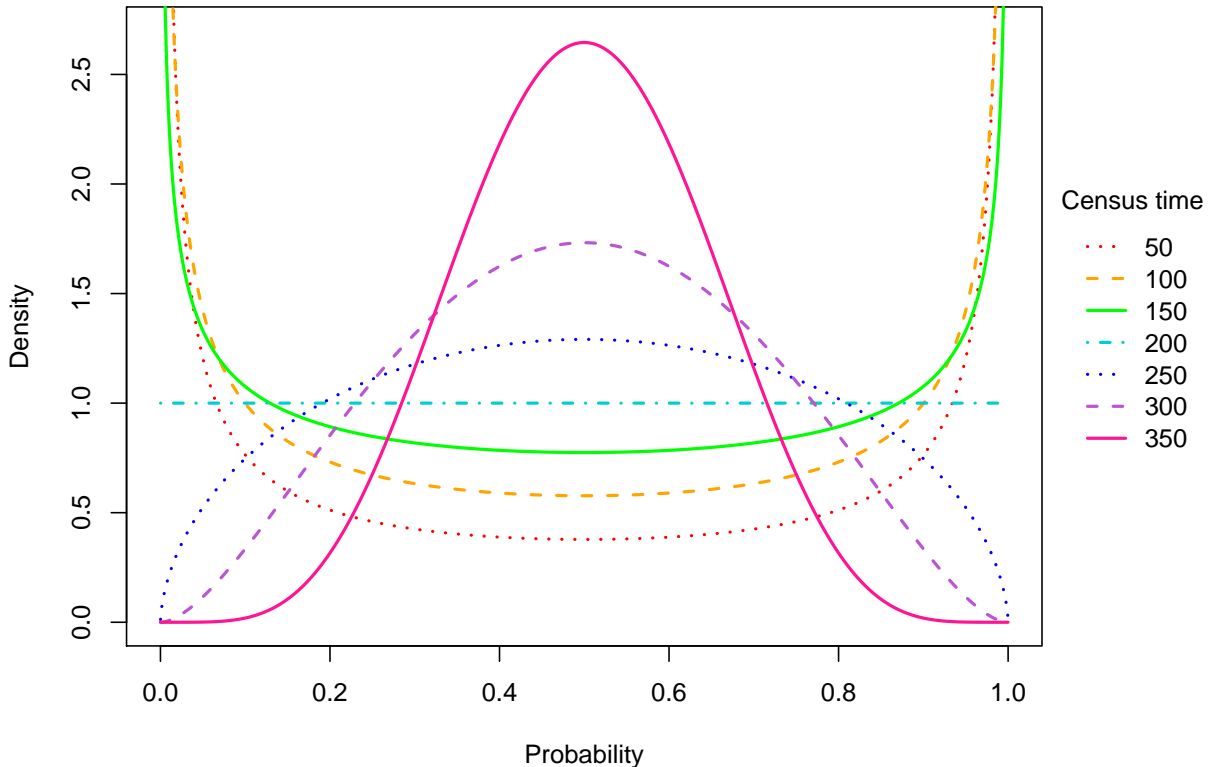


Figure 1: Theoretical density of $\mathbb{P}(N_{\bullet}^+ \leq \hat{q}_{0.5})$ as a function of census time, t , with $t^+ = 400 - t$, $\alpha = 2$, $\beta = 150$ and $C = 150$.

Despite this decidedly unintuitive behaviour of the quantile probabilities, Theorem 1 also shows that the relative error in the quantile estimate decays with C in the expected way. The resolution of this apparent contradiction lies in the fact that whilst the quantiles for N_{\bullet}^+ and \tilde{N}_{\bullet}^+ themselves are $\mathcal{O}(C)$, both the discrepancy between them *and* the widths of

the distributions are $\mathcal{O}(\sqrt{C})$. The discrepancy between the quantiles also decreases to 0 as $t^+/t \downarrow 0$, so depending on this ratio the two distributions can closely overlap or almost entirely diverge ($t^+ \gg t$).

Thus, even though the point estimate of a quantile may be accurate relative to the size of the quantile ($\mathcal{O}(\sqrt{C})$ compared with $\mathcal{O}(C)$), unless $t^+ \ll t$, prediction intervals will not, in general, provide the intuitive and desirable coverage properties: $\mathbb{P}(\hat{q}_{0.05} \leq N_{\bullet}^+ \leq \hat{q}_{0.95}) \approx 0.9$, for example. However, the (asymptotically) correct coverage can be recovered by adjusting the interval, based on Theorem 1, as we now describe.

Theorem 1 suggests that to obtain a predictive value with the true (asymptotic in C) probability p of it not being exceeded, we must target a value p^* such that

$$p = \mathbb{E} \left[\Phi \left(\sqrt{\frac{t^+}{t}} Z + \Phi^{-1}(p^*) \sqrt{\frac{\beta + t + t^+}{\beta + t}} \right) \right].$$

Writing b for $\Phi^{-1}(p^*) \sqrt{(\beta + t + t^+)/(\beta + t)}$ and letting $Z' \sim \mathbf{N}(0, 1)$ be independent of Z , the right hand side may be rewritten as

$$\mathbb{P} \left(Z' \leq \sqrt{\frac{t^+}{t}} Z + b \right) = \mathbb{P} \left(\sqrt{1 + \frac{t^+}{t}} \mathbf{N}(0, 1) \leq b \right) = \Phi \left(\frac{b}{\sqrt{1 + \frac{t^+}{t}}} \right).$$

Rearranging gives

$$\sqrt{\frac{t + t^+}{t}} \Phi^{-1}(p) = \sqrt{\frac{\beta + t + t^+}{\beta + t}} \Phi^{-1}(p^*),$$

so

$$p^* = \Phi \left(\sqrt{\frac{(\beta + t)(t + t^+)}{t(\beta + t + t^+)}} \Phi^{-1}(p) \right). \quad (7)$$

In practice we substitute $\hat{\beta}$ for β .

3.2 Different centre opening times

We now consider the scenario where $t_1 = \dots = t_c$ does not hold. In this case the posterior for λ_{\bullet} is intractable and, hence, so are the distributions for \tilde{N}_{\bullet}^+ and \tilde{T}^+ . Furthermore, Lemma 1 does not hold.

Although the distribution of λ_{\bullet} is intractable, its moments are not:

$$\mathbb{E}[\lambda_{\bullet}] = \sum_{c=1}^C \frac{\hat{\alpha} + n_c}{\hat{\beta} + t_c} \quad \text{and} \quad \text{Var}[\lambda_{\bullet}] = \sum_{c=1}^C \frac{\hat{\alpha} + n_c}{(\hat{\beta} + t_c)^2}.$$

We make the intuitive approximation that

$$\lambda_{\bullet} \stackrel{D}{\approx} \lambda_{\bullet}^* \sim \text{Gam}(C\hat{\alpha} + n_{\bullet}^*, \hat{\beta} + t^*),$$

where n_{\bullet}^* and t^* are chosen so that the first two moments of λ_{\bullet}^* match those of λ_{\bullet} . Figure 5 in the appendix, and the accompanying text, demonstrate the accuracy of this approximation for two scenarios relevant to trial recruitment that we will describe in Section 4.2.

This is exactly the posterior distribution for λ_{\bullet}^* that would arise given the $\text{Gam}(C\hat{\alpha}, \hat{\beta})$ prior if each centre had been open for the same time of t^* and the total recruited had been n_{\bullet}^* patients. Thus, if the MLEs from this ‘data’, $\hat{\alpha}^*$ and $\hat{\beta}^*$ were to satisfy $\hat{\alpha}^* = \hat{\alpha}$ and $\hat{\beta}^* = \hat{\beta}$ then the theory from Section 3.1 would follow through exactly. In reality, whatever the partitioning of n_{\bullet}^* across centres, the data would typically lead to slightly different MLEs $\hat{\alpha}^* \neq \hat{\alpha}$ and $\hat{\beta}^* \neq \hat{\beta}$; nevertheless, in the proof of Theorem 1 the most important aspect of the MLEs is their ratio. From Lemma 1, $\hat{\alpha}^*/\hat{\beta}^* = n_{\bullet}^*/Ct^*$, and empirical comparisons of n_{\bullet}^*/Ct^* against $\hat{\alpha}/\hat{\beta}$ (see Figure 6 in the Appendix) showed a relative error of less than 0.1%.

The methodology for constructing prediction intervals for either \tilde{N}_{\bullet}^+ or \tilde{T}^+ then proceeds as in Section 3.1, using $\hat{\alpha}$ and $\hat{\beta}$ under the assumption that $\lambda_{\bullet} \equiv \lambda_{\bullet}^*$.

4 Empirical verification of theory and methodology

Simulations were carried out to test the asymptotic theory and methods proposed in this paper for finite numbers of centres, C . A large number (20000 unless otherwise stated) of realisations of the parameters $\lambda_1, \dots, \lambda_C$, and hence the sample (n_1, \dots, n_C) were simulated for a given set of parameter values. For each realisation, the parameters α and β were estimated using maximum likelihood and the quantile of interest, \hat{q}_p for either N_{\bullet}^+ or T^+ was estimated. Either $\mathbb{P}(N_{\bullet}^+ \leq \hat{q}_p)$ or $\mathbb{P}(T^+ \leq \hat{q}_p)$ was then calculated exactly using the known (simulated) $\lambda_1, \dots, \lambda_C$. The results outlined below will primarily focus on predicting N_{\bullet}^+ .

Unless specified otherwise, the following parameter values were used: $\alpha = 2$, $\beta = 150$. A default number of centres of $C = 150$ was used when the census time, t , was varied, and a default of $t = 200$ was used when C was varied. When predicting N_{\bullet}^+ , the total trial length was set to $\tau = t + t^+ = 400$, since with the default C , $\mathbb{E}[N_{\bullet} + N_{\bullet}^+] = C(\alpha/\beta)(t + t^+) = 800$, a reasonable size for a Phase III clinical trial. Furthermore, the census time t was chosen from $\mathbb{T}_1 = \{50, 100, 150, 200, 250, 300, 350\}$ and the number of centres, C , was chosen from $\mathbb{C}_1 = \{20, 50, 100, 150, 200, 250, 300, 400\}$. When examining predictions of T^+ we fixed $n^+ = 200$ and selected $T \in \mathbb{T}_2 = \{50, 100, 150, 200, 300, 500, 1000\}$ and $C \in \mathbb{C}_2 = \{20, 50, 100, 150, 200, 300, 500, 1000\}$.

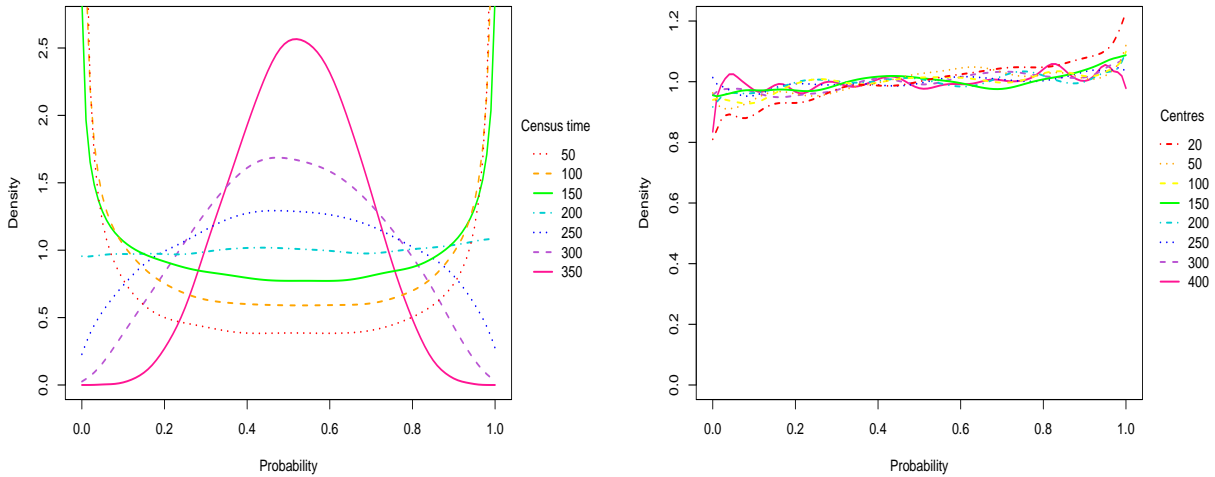


Figure 2: Estimated density (over repeated sampling) of $\mathbb{P}(N_{\bullet}^+ \leq \hat{q}_{0.5})$ for each $t \in \mathbb{T}_1$ with $t^+ = 400 - t$ (left) and for each $C \in \mathbb{C}_1$ with $t = t^+ = 200$ (right).

4.1 Verification of Theorem 1

Figure 2 shows the empirical distribution of $\mathbb{P}(N_{\bullet}^+ \leq \hat{q}_p)$ over repeated simulated data sets and, hence, estimates \hat{q}_p , for the median, $p = 0.5$. The left panel varies the census times $t \in \mathbb{T}_1$, whilst the right panel fixes t (and hence $t^+ = \tau - t$) and varies the number of centres, $C \in \mathbb{C}_1$. The shape of the density function for $\mathbb{P}(N_{\bullet}^+ \leq \hat{q}_p)$ depends on the ratio of t^+/t and shows very little variation with C , just as described in Section 3.1, and matching almost perfectly the relevant theoretical curves in Figure 1. In particular, when $t = t^+$, as in all cases in the right panel, the distribution is very close to uniform, empirically verifying the, perhaps unintuitive, result that increasing the number of centres in the trial, thus increasing the sample size upon which the MLEs are based, does not affect the accuracy of the quantile estimates.

Figure 3 repeats Figure 1 and the left panel of Figure 2 but for the $p = 0.25$ quantile. Again, the empirical results match the theory almost perfectly. As with $p = 0.5$, the estimate improves with increasing census time, but as predicted in Section 3.1, when $t \ll t^+$, the mass is now not evenly distributed between the regions close to 0 and close to 1.

When predicting quantiles for T^+ , Theorem 1 suggests that the accuracy of the quantile is primarily dependent on the ratio of $n_{\bullet}^+/n_{\bullet}$. Thus with a fixed n_{\bullet}^+ , the transition of the density curves for $\mathbb{P}(T^+ \leq \hat{q}_p)$ from a point mass at p to a concentration at 0 and 1, occurs as the number of centres increases and as the census time increases, since each of these increases n . The observed effect of the number of centres on the accuracy of the predicted median compares well with the theoretically predicted densities (Figure 4). For further validation,

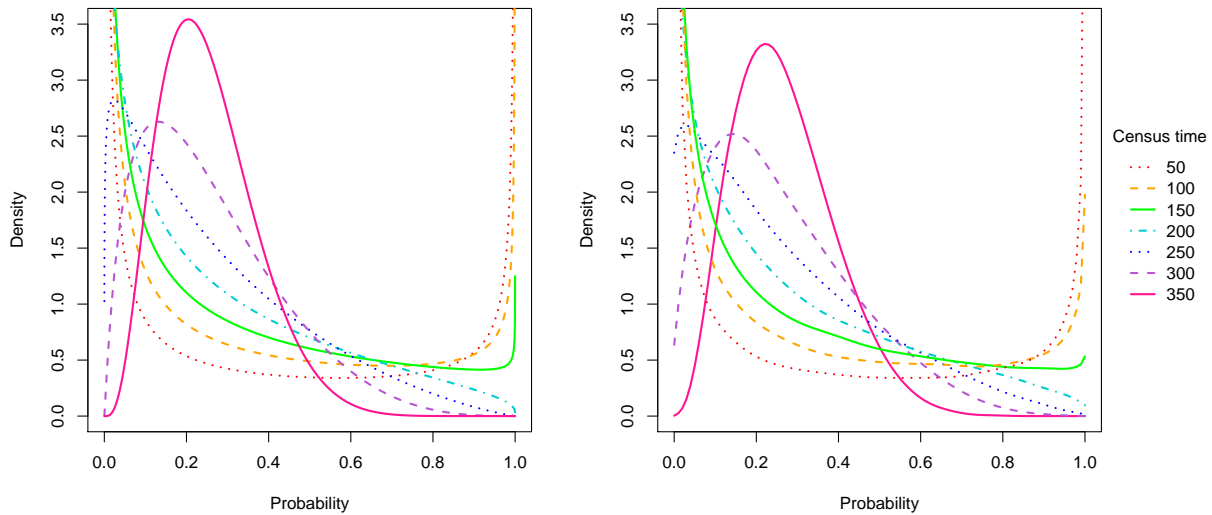


Figure 3: Theoretical density (left) and estimated density over repeated sampling (right) of $\mathbb{P}(N_{\bullet}^+ \leq \hat{q}_{0.25})$ for each $t \in \mathbb{T}_1$, with $t^+ = 400 - t$.

corresponding plots for $p = 0.25$ with t varying are provided in the appendix.

4.2 Adjusted prediction intervals

We now study empirically the effectiveness of using quantiles based on $p^*(p)$ to derive prediction intervals, and compare with intervals based directly on p . At each simulation, a standard, unadjusted 90% interval was estimated by calculating \hat{q}_p for $p = 0.05$ and $p = 0.95$. An adjusted 90% interval was also derived by using $p^*(p)$ from (7) instead of p , both for $p = 0.05$ and $p = 0.95$. The performance of the intervals was assessed for each method by calculating the mean, over 2000 simulations, of the true prediction interval coverage (calculated using the simulated $\lambda_1, \dots, \lambda_C$). The mean width of the prediction intervals was also recorded. We first consider the case where all centres opened simultaneously, then the case of different centre opening times.

All centres opened simultaneously. Table 1 shows the results for each $t \in \mathbb{T}_1$, and $t^+ = \tau - t$. The unadjusted method gives satisfactory results for $t \ll t^+$ only, as is to be expected given Theorem 1. For all other scenarios, the quantiles are inaccurately estimated and the coverage can be far less than intended, as low as 63.7% for a census time early on in the trial. Further diagnostics showed approximately equal contributions to undercoverage from $\hat{q}_{0.05}$ being too high and $\hat{q}_{0.95}$ being too low. In contrast, by applying (7), the coverage is consistently improved upon and corrected to almost exactly the desired 90%. The improved coverage does come with a cost of an increased interval width, but the increase seems

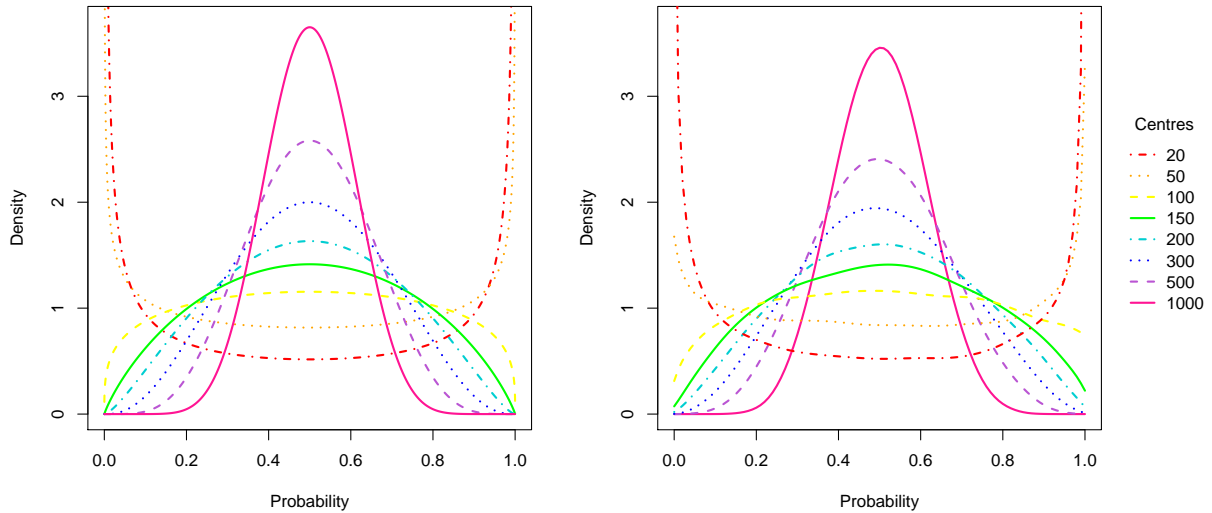


Figure 4: Theoretical density (left) and estimated density over repeated sampling (right) of $\mathbb{P}(T^+ \leq \hat{q}_{0.5})$ for each $C \in \mathbb{C}_2$ with $n_{\bullet}^+ = 200$ fixed across all simulation runs.

proportionate.

Table 1: The mean (over repeated sampling) of the true coverage probability and width of an intended 90% prediction interval for N_{\bullet}^+ using the unadjusted and adjusted methods.

	Unadjusted		Adjusted	
	Coverage (%)	w	Coverage (%)	w
$t = 50, t^+ = 350$	63.7	140.5	89.1	245.6
$t = 100, t^+ = 300$	76.3	118.2	89.5	160.9
$t = 150, t^+ = 250$	81.9	99.0	89.5	120.0
$t = 200, t^+ = 200$	84.9	82.2	89.6	92.9
$t = 250, t^+ = 150$	86.9	66.6	89.8	72.0
$t = 300, t^+ = 100$	88.2	51.3	89.8	53.6
$t = 350, t^+ = 50$	89.2	34.5	89.9	35.1

When $\beta = 0$, (7) gives $p^* = p$: no correction is needed. We, therefore, also examined the effect of our adjustment when data are simulated using a much lower true parameter value, $\beta = 50$. In this case, the lowest coverage ($t = 50, t^+ = 350$) was 77.8%, improving to 90.2% after our adjustment, whilst when $t = t^+ = 200$ the coverage improved from 84.1% to 90.0%; the full tabulation is provided in the appendix.

Similar improvements to those in Table 1, but for the 95% prediction interval are provided in the appendix, confirming that the p^* adjustment performs equally well when adjusting quantiles which are further into the tails of the distribution. A further table in the appendix

demonstrates the even more striking improvements than in Table 1, found when creating a 90% predictive interval but with $C = 20$; for example, when $(t, t^+) = (50, 350)$ the coverage improved from 59.2% to 89.7%.

Different centre opening times. We consider two different opening time scenarios: (1) the centre opening times are drawn uniformly and independently from the interval $[0, t]$, and (2) half of the centres are opened at time 0 and half of the centres open at time t . The former mimics a gradual coming online of new centres, whilst the latter scenario could occur when an initial interim analysis suggests that many new centres must be opened to achieve the required sample size.

The investigation into quantile adjustment to obtain a 90% prediction interval (Table 1) was repeated for opening-time scenarios (1) and (2), and the results are provided in Tables 2 and 3, respectively. The prediction intervals for these cases were constructed according to the methodology of Section 3.2. Additional diagnostics for the moment matching approach were also recorded: the mean (over repeated samples) of t^* , the ratio of this to the mean (over repeated samples) of the mean (over centres) of the t_c 's, and the ratio of the mean of the n_\bullet^* to the mean of the n_\bullet .

In both cases, the intervals obtained by combining the methodology proposed in Section 3.2 with (7) produce coverages very close to 90%, whatever the census time. By contrast the unadjusted intervals suffered from coverages as low as 50% when $t = 50$. Typically the values of t^* and n_\bullet^* are lower than t and n_\bullet (although their ratio is almost unchanged; see Section 3.2), representing the increased uncertainty in parameter values because some centres have not been open for the full time interval. The especially poor coverage of the standard intervals results because it is now the ratio t^+/t^* that determines the extent of the undercoverage.

Table 2: The mean (over repeated sampling) of the true coverage probability and width of an intended 90% prediction interval for N_\bullet^+ using the unadjusted and adjusted methods for opening time Scenario 1.

				Unadjusted		Adjusted	
	t^*	t^*/t_c	n_\bullet^*/n_\bullet	Coverage (%)	w	Coverage (%)	w
$t = 50, t^+ = 350$	23.9	0.955	0.954	50.5	144.0	89.6	344.0
$t = 100, t^+ = 300$	46.1	0.920	0.919	64.7	125.1	89.8	220.9
$t = 150, t^+ = 250$	66.8	0.890	0.890	71.8	106.5	89.6	160.1
$t = 200, t^+ = 200$	86.6	0.865	0.865	77.2	88.7	89.6	119.7
$t = 250, t^+ = 150$	105.6	0.844	0.843	81.1	71.4	89.7	88.7
$t = 300, t^+ = 100$	123.9	0.825	0.825	84.4	54.2	89.8	62.5
$t = 350, t^+ = 50$	141.8	0.810	0.809	87.2	35.5	89.9	38.2

Equivalent tables for T^+ for Scenarios 1 and 2, presented in the appendix, show similar

Table 3: The mean (over repeated sampling) of the true coverage probability and width of an intended 90% prediction interval for N_{\bullet}^+ using the unadjusted and adjusted method for opening time Scenario 2.

	t^*	t^*/t_c	$n_{\bullet}^*/n_{\bullet}$	Unadjusted		Adjusted	
				Coverage (%)	w	Coverage (%)	w
$t = 50, t^+ = 350$	21.6	0.863	0.860	47.5	146.3	89.8	361.3
$t = 100, t^+ = 300$	38.0	0.761	0.758	60.9	127.7	90.2	240.8
$t = 150, t^+ = 250$	50.8	0.678	0.675	67.8	109.2	90.2	179.5
$t = 200, t^+ = 200$	61.1	0.611	0.608	72.5	91.3	89.9	136.5
$t = 250, t^+ = 150$	69.8	0.558	0.555	75.9	73.6	89.4	101.5
$t = 300, t^+ = 100$	76.6	0.511	0.508	80.0	55.7	89.7	70.8
$t = 350, t^+ = 50$	82.4	0.471	0.469	84.5	36.2	89.9	41.8

dramatic improvements.

5 Proof of Theorem 1

In this section, since all quantities are totals, we simplify the notation, altering λ_{\bullet} to λ , N_{\bullet} to N , N_{\bullet}^+ to N^+ and \tilde{N}_{\bullet}^+ to \tilde{N}^+ . Further, since $\lambda \sim \text{Gam}(C\alpha, \beta)$ and $N|\lambda \sim \text{Po}(\lambda t)$, Chebyshev's inequality gives: $\lambda t/C \xrightarrow{p} t\alpha/\beta$ and $N/(\lambda t) \xrightarrow{p} 1$, and hence $N/C \xrightarrow{p} t\alpha/\beta$; finally, by the Central Limit Theorem (CLT):

$$(N - \lambda t)/\sqrt{\lambda t} \Rightarrow Z \sim \text{N}(0, 1). \quad (8)$$

We prove Parts 1 and 2 of the theorem separately. In each case we initially condition on the random variable (λ, \underline{N}) ; however, the final, limiting probability quantity depends on this random variable only through Z .

5.1 Proof of Part 1

Combining Lemma 1 with (4) gives

$$\mathbb{E}[\tilde{N}^+ | \underline{N}] = \frac{Nt^+}{t} \quad \text{and} \quad \text{Var}[\tilde{N}^+ | \underline{N}] = \frac{Nt^+}{t} \times \frac{\hat{\beta} + t + t^+}{\hat{\beta} + t}. \quad (9)$$

Moreover, (9) gives

$$\frac{\text{Var}[\tilde{N}^+ | \underline{N}]}{\text{Var}[N^+ | \lambda]} = \frac{N}{\lambda t} \times \frac{\hat{\beta} + t + t^+}{\hat{\beta} + t} \xrightarrow{p} \frac{\beta + t + t^+}{\beta + t}, \quad (10)$$

since $\widehat{\beta} \xrightarrow{p} \beta$ by the asymptotic consistency of the MLE.

Conditional on N , let $\widetilde{N}_c^+ \sim \mathbf{NB}\left(\widehat{\alpha} + N/C, \frac{t^+}{\beta + t + t^+}\right)$ be independent. Then $\widetilde{N}^+ \stackrel{D}{=} \sum_{c=1}^C \widetilde{N}_c^+$. Also $N^+ | \lambda \sim \text{Po}(\lambda t^+)$, so as $C \rightarrow \infty$, which implies $N/C \xrightarrow{p} t\alpha/\beta$, the CLT gives

$$(N^+ - \lambda t^+) / \sqrt{\lambda t^+} | \lambda \Rightarrow \mathbf{N}(0, 1), \quad (11)$$

$$(\widetilde{N}^+ - \mathbb{E}[\widetilde{N}^+ | \underline{N}]) / \sqrt{\text{Var}[\widetilde{N}^+ | \underline{N}]} | \underline{N} \Rightarrow \mathbf{N}(0, 1). \quad (12)$$

Substituting (8) into (9)

$$\frac{\mathbb{E}[\widetilde{N}^+ | \underline{N}] - \mathbb{E}[N^+ | \lambda]}{\sqrt{\text{Var}[N^+ | \underline{N}]}} \Rightarrow \frac{\frac{t^+}{t}(\lambda t + \sqrt{\lambda t} Z) - \lambda t^+}{\sqrt{\lambda t^+}} = \sqrt{\frac{t^+}{t}} Z.$$

Incorporating this with (12) and (10), the prediction of the p th quantile, \hat{q}_p , satisfies

$$\begin{aligned} \frac{\hat{q}_p - \mathbb{E}[N^+ | \lambda]}{\sqrt{\text{Var}[N^+ | \lambda]}} | N \xrightarrow{p} & \frac{\mathbb{E}[\widetilde{N}^+ | \underline{N}] - \mathbb{E}[N^+ | \lambda] + \Phi^{-1}(p) \sqrt{\text{Var}[\widetilde{N}^+ | \underline{N}]}}{\sqrt{\text{Var}[N^+ | \lambda]}} \\ & \Rightarrow \sqrt{\frac{t^+}{t}} Z + \Phi^{-1}(p) \sqrt{\frac{\beta + t + t^+}{\beta + t}}. \end{aligned} \quad (13)$$

From (11) and (13), the probability the true realisation is less than the predicted quantile is

$$\mathbb{P}(N^+ \leq \hat{q}_p | \underline{N}, \lambda) \xrightarrow{p} \Phi\left(\frac{\hat{q}_p - \mathbb{E}[N^+ | \lambda]}{\sqrt{\text{Var}[N^+ | \lambda]}}\right) \Rightarrow \Phi\left(\sqrt{\frac{t^+}{t}} Z + \Phi^{-1}(p) \sqrt{\frac{\beta + t + t^+}{\beta + t}}\right).$$

Since this does not depend on λ , it is also the limit of $\mathbb{P}(N^+ \leq \hat{q}_p | \underline{N})$, as required. Furthermore, from (13) and (11), the discrepancy between the quantile approximation and the true quantile satisfies

$$\frac{\hat{q}_p - q_p}{\sqrt{\text{Var}[N^+ | \lambda]}} \approx \sqrt{\frac{t^+}{t}} Z + \Phi^{-1}(p) \left[\sqrt{\frac{\beta + t + t^+}{\beta + t}} - 1 \right] = \mathcal{O}(\sqrt{t^+/t})$$

for small t^+ . Since since $q_p/C \rightarrow \alpha/\beta$ and $\text{Var}[N^+ | \lambda] = \mathcal{O}(C)$, the second result follows.

5.2 Proof of Part 2

Firstly, since $T^+ | \lambda \sim \text{Gam}(n^+, \lambda)$,

$$\mathbb{E}[T^+ | \lambda] = \frac{n^+}{\lambda} = \frac{n^+/C}{\lambda/C} \xrightarrow{p} \frac{a\beta}{\alpha} \quad \text{and} \quad C\text{Var}[T^+ | \lambda] = C \frac{n^+}{\lambda^2} \xrightarrow{p} \frac{a\beta^2}{\alpha^2}. \quad (14)$$

Combining Lemma 1 with (6) and using the asymptotic consistency of the MLEs,

$$\mathbb{E} \left[\tilde{T}^+ \mid \underline{N} \right] = \frac{(\hat{\beta} + t)n^+}{C\hat{\alpha} + N - 1} = \frac{(\hat{\beta} + t)n^+t}{(\hat{\beta} + t)N - t} \xrightarrow{p} \frac{a\beta}{\alpha}. \quad (15)$$

$$\begin{aligned} C\text{Var} \left[\tilde{T}^+ \mid \underline{N} \right] &= \mathbb{E} \left[\tilde{T}^+ \mid \underline{N} \right] \times \frac{(\hat{\beta} + t)(\hat{\alpha} + N/C + n^+/C - 1/C)}{(\hat{\alpha} + N/C - 1/C)(\hat{\alpha} + N/C - 2/C)} \\ &\xrightarrow{p} \frac{a\beta}{\alpha} \times \frac{(\beta + t)(\alpha + \alpha t/\beta + a)}{(\alpha + \alpha t/\beta)^2} \\ &= \frac{a\beta^2(1 + a/\alpha + t/\beta)}{\alpha^2(1 + t/\beta)}. \end{aligned}$$

Thus

$$\frac{\text{Var} \left[\tilde{T}^+ \mid \underline{N} \right]}{\text{Var} \left[T^+ \mid \lambda \right]} \xrightarrow{p} \frac{1 + a/\alpha + t/\beta}{1 + t/\beta}. \quad (16)$$

Also, from the second equality in (15),

$$\begin{aligned} \frac{\mathbb{E} \left[\tilde{T}^+ \mid \underline{N} \right] - \mathbb{E} \left[T^+ \mid \lambda \right]}{\sqrt{\text{Var} \left[T^+ \mid \lambda \right]}} &= \frac{1}{\sqrt{n^+/\lambda^2}} \times \left[\frac{(\hat{\beta} + t)n^+t}{(\hat{\beta} + t)N - t} - \frac{n^+}{\lambda} \right] \\ &= \sqrt{n^+} \left[\frac{(\hat{\beta} + t)(\lambda t - N) + t}{(\hat{\beta} + t)N - t} \right] \\ &= \sqrt{\frac{n^+/C}{\lambda t/C}} \left[\frac{(\hat{\beta} + t)(\lambda t - N)/\sqrt{\lambda t} + t/\sqrt{\lambda t}}{(\hat{\beta} + t)N/(\lambda t) - t/(\lambda t)} \right] \\ &\Rightarrow -\sqrt{\frac{a\beta}{\alpha t}} \times Z, \end{aligned} \quad (17)$$

by (8). Now $\lambda T^+ \sim \text{Gam}(n^+, 1) = \sum_{i=1}^{n^+} E_i$, where the $E_i \sim \text{Exp}(1)$ are independent and identically distributed, so the central limit theorem gives

$$\frac{T^+ - \mathbb{E} \left[T^+ \mid \lambda \right]}{\sqrt{\text{Var} \left[T^+ \mid \lambda \right]}} = \frac{\lambda T^+ - \mathbb{E} \left[\lambda T^+ \mid \lambda \right]}{\sqrt{\text{Var} \left[\lambda T^+ \mid \lambda \right]}} \Rightarrow \mathbf{N}(0, 1).$$

Further, $\tilde{T}^+ \mid \underline{N} \stackrel{D}{=} \text{Gam}(n^+, 1)/\lambda \mid \underline{N} = G_1/G_2$, where $G_1 \sim \text{Gam}(n^+, 1)$ and $G_2 \sim \text{Gam}(C\hat{\alpha}, \hat{\beta})$ are independent. Since $n^+ \rightarrow \infty$ as $C \rightarrow \infty$ and the MLEs are consistent, the delta method and the CLT give: $(\tilde{T}^+ - \mathbb{E} \left[\tilde{T}^+ \mid \underline{N} \right])/\sqrt{\text{Var} \left[\tilde{T}^+ \mid \underline{N} \right]} \mid \underline{N} \Rightarrow \mathbf{N}(0, 1)$. Hence,

$$\begin{aligned} \mathbb{P} \left(T^+ \leq \hat{q}_p \mid \underline{N}, \lambda \right) &\xrightarrow{p} \Phi \left(\frac{\mathbb{E} \left[T \right] + \Phi^{-1}(p)\sqrt{\text{Var} \left[\tilde{T}^+ \right]} - \mathbb{E} \left[T^+ \right]}{\sqrt{\text{Var} \left[T^+ \right]}} \right) \\ &\Rightarrow \Phi \left(-\sqrt{\frac{a\beta}{\alpha t}} Z + \Phi^{-1}(p)\sqrt{\frac{1 + a/\alpha + t/\beta}{1 + t/\beta}} \right). \end{aligned}$$

As with the proof of Part 1, this does not depend on λ so is also the limit of $\mathbb{P}(T^+ \leq q_p \mid \underline{N})$. Finally, from (14), (16), (17) and the two CLT applications above,

$$\frac{\hat{q}_p - q_p}{\sqrt{\text{Var}[T^+ \mid \lambda]}} \approx -\sqrt{\frac{a\beta}{\alpha t}} \times Z + \Phi^{-1}(p) \left\{ \sqrt{\frac{1 + t/\beta + a/\alpha}{1 + t/\beta}} - 1 \right\}$$

Since $\text{Var}[T^+ \mid \lambda] = \mathcal{O}(a/C)$ and $q_p = \mathcal{O}(a)$ the second part follows.

Acknowledgements: The first author acknowledges support from award: NIHR-MS-2016-03-01 Lancaster University.

References

- [1] A. K. Akobeng. Understanding randomised controlled trials. *Archives of Disease in Childhood*, 90(8):840–844, 2005.
- [2] Rickey E. Carter. Application of stochastic processes to participant recruitment in clinical trials. *Controlled Clinical Trials*, 25(5):429 – 436, 2004.
- [3] Benjamin Carlisle, Jonathan Kimmelman, Tim Ramsay, and Nathalie MacKinnon. Unsuccessful trial accrual and human subjects protections: An empirical analysis of recently closed trials. *Clinical Trials*, 12(1):77–83, 2015. PMID: 25475878.
- [4] Mary Jo Lamberti, Adam Mathias, Jane E. Myles, Deborah Howe, and Ken Getz. Evaluating the impact of patient recruitment and retention practices. *Drug Information Journal*, 46(5):573–580, 2012.
- [5] Grant D. Huang, Jonca Bull, Kelly J. McKee, Elizabeth Mahon, Beth Harper, and Jamie N. Roberts. Clinical trials recruitment planning: A proposed framework from the clinical trials transformation initiative. *Contemporary Clinical Trials*, 66:74 – 79, 2018.
- [6] Shaun Treweek, Pauline Lockhart, Marie Pitkethly, Jonathan A Cook, Monica Kjeldstrøm, Marit Johansen, Taina K Taskila, Frank M Sullivan, Sue Wilson, Catherine Jackson, Ritu Jones, and Elizabeth D Mitchell. Methods to improve recruitment to randomised controlled trials: Cochrane systematic review and meta-analysis. *BMJ Open*, 3(2), 2013.
- [7] Rickey E. Carter, Susan C. Sonne, and Kathleen T. Brady. Practical considerations for estimating clinical trial accrual periods: application to a multi-center effectiveness study. *BMC Medical Research Methodology*, 5(1), 2005.
- [8] Stephen Senn. *Statistical issues in drug development*. Statistics in practice (Chichester, England). John Wiley, Chichester ; New York, 1997.

- [9] Gong Tang, Yuan Kong, Chung-Chou Ho Chang, Lan Kong, and Joseph P. Costantino. Prediction of accrual closure date in multi-center clinical trials with discrete-time poisson process models. *Pharmaceutical Statistics*, 11(5):351356, 2012.
- [10] Yu Lan, Gong Tang, and Daniel F. Heitjan. Statistical modelling and prediction of clinical trial recruitment. *Statistics in Medicine*, 38(6):945–955, 2019.
- [11] Vladimir V. Anisimov and Valerii V. Fedorov. Modelling, prediction and adaptive adjustment of recruitment in multicentre trials. *Statistics in Medicine*, 26(27):49584975, 2007.
- [12] Andisheh Bakhshi, Stephen Senn, and Alan Phillips. Some issues in predicting patient recruitment in multi-centre clinical trials. *Statistics in Medicine*, 32(30):5458–5468, 2013.
- [13] Guillaume Mijoule, Stphanie Savy, and Nicolas Savy. Models for patients’ recruitment in clinical trials and sensitivity analysis. *Statistics in Medicine*, 31(16):1655–1674, 2012.
- [14] Szymon Urbas, Chris Sherlock, and Paul Metcalfe. Interim recruitment prediction for multi-centre clinical trials, 2019.
- [15] Ismail Abbas, Joan Rovira, and Josep Casanovas. Clinical trial optimization: Monte carlo simulation markov model for planning clinical trials recruitment. *Contemporary Clinical Trials*, 28(3):220 – 231, 2007.
- [16] Anna-Bettina Haidich and John Pa Ioannidis. Determinants of patient recruitment in a multicenter clinical trials group: trends, seasonality and the effect of large studies. *BMC Medical Research Methodology*, 1(1), Jun 2001.
- [17] Dejian Lai, Lemuel A. Moy, Barry R. Davis, Lisa E. Brown, and Frank M. Sacks. Brownian motion and long-term clinical trial recruitment. *Journal of Statistical Planning and Inference*, 93(1):239 – 246, 2001.
- [18] Qiang Zhang and Dejian Lai. Fractional brownian motion and long term clinical trial recruitment. *Journal of Statistical Planning and Inference*, 141(5):1783 – 1788, 2011.
- [19] Gui-shuang Ying. *Prediction of event times in randomized clinical trials*. PhD thesis, University of Pennsylvania, 2004.
- [20] Norman L. Johnson, Samuel Kotz, and N. Balakrishnan. *Continuous univariate distributions*. Wiley series in probability and mathematical statistics. Wiley, New York, 2nd ed. edition, 1994.

A Supplementary material for Section 3.2

Figures 5 and 6 support the use of the theory proposed in Section 3.2. Figure 5 shows the accuracy of the moment matched gamma distribution to estimate the distribution of λ_{\bullet} , as well as a CLT-based Gaussian approximation, using rates arising from Opening Time Scenario 1. The moment-matched gamma performs very well, and is superior to the CLT for small number of centres, whilst both are very accurate for large C . The Gaussian approximation is purely present for comparison, since a gamma distribution is required for tractability of the integrals over λ_{\bullet} , both for \tilde{N}_{\bullet}^+ and \tilde{T}^+ . Plots for Opening Time Scenario 2 (not included) show a similarly good fit. Figure 6 provides an empirical comparison of $\hat{\alpha}/\hat{\beta}$ against n^*/Ct^* for the two opening time scenarios. The plots support the use of the MLEs from the original data, to a data set where n_{\bullet}^* patients have been recruited in time t^* , as outlined in Section 3.2.

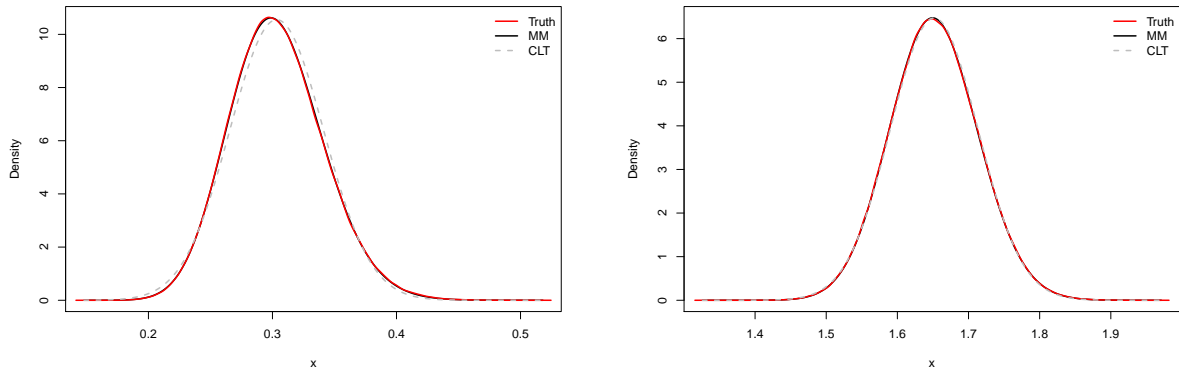


Figure 5: Comparison of using the moment matched (MM) method and the central limit theorem (CLT) to estimate the sum of gamma random variables with different rate parameters, from Opening Time Scenario 1, with $C = 20$ (left) / $C = 150$ (right), $\alpha = 2$, $\beta = 150$ and $t = 200$.

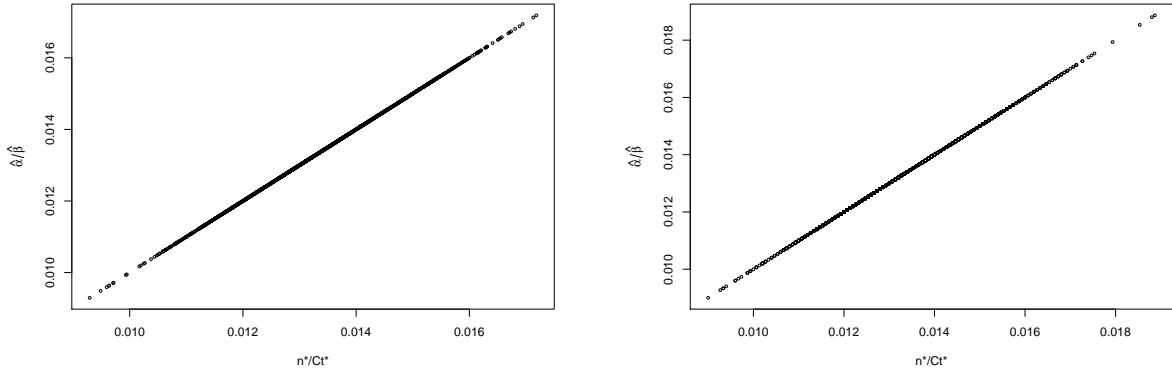


Figure 6: Plot of $\hat{\alpha}/\hat{\beta}$ against n^*/Ct^* for centre opening time scenario 1 (left) and scenario 2 (right) with $\alpha = 2$, $\beta = 150$, $C = 150$ and $t = 200$.

B Additional results for Section 4.1

Figure 7 provides further validation of Theorem 1 for T^+ . The accuracy of the $p = 0.25$ quantile is primarily dependent on the ratio of $n_{\bullet}^+/n_{\bullet}$, hence for a fixed n_{\bullet}^+ , the density concentrates at the point mass p with increasing census time. The observed effect of the census time on the accuracy of the predicted quantile compares well with the theoretical densities.

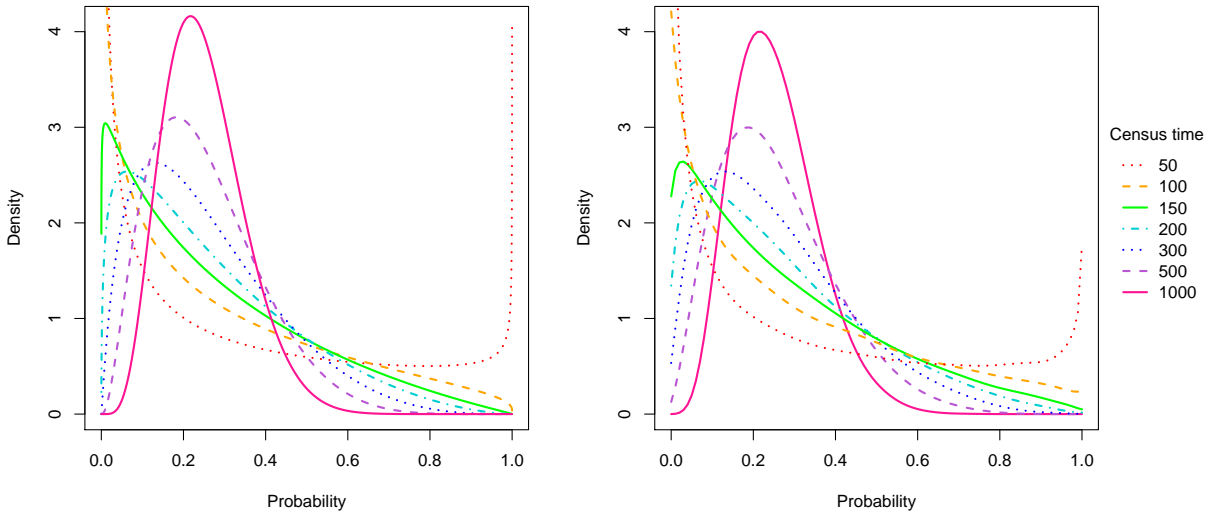


Figure 7: Theoretical density (left) and estimated density over repeated sampling (right) of $\mathbb{P}(T^+ \leq \hat{q}_{0.25})$ for each $t \in \mathbb{T}_2$ with $n_{\bullet}^+ = 200$ fixed across all simulation runs.

C Additional results for Section 4.2

The results tables in this section evidence further investigation into the interval adjustment methodology.

Table 4 shows that the methodology is still helpful for creating prediction intervals for N_{\bullet}^+ when β is 50 rather than 150. Tables 5 and 6 correspond to $\beta = 150$ but, respectively examining 95% intervals or 90% intervals with $C = 20$. The remaining tables display results of interval adjustment for T^+ for each of the three centre opening time scenarios considered.

Table 4: The mean (over repeated sampling) of the true coverage probability and width of an intended 90% prediction interval for N_{\bullet}^+ with $\beta = 50$ using the unadjusted and adjusted method.

	Unadjusted		Adjusted	
	Coverage (%)	w	Coverage (%)	w
$t = 50, t^+ = 350$	77.8	317.1	90.2	426.5
$t = 100, t^+ = 300$	84.8	240.7	90.2	278.8
$t = 150, t^+ = 250$	86.2	190.7	89.4	207.9
$t = 200, t^+ = 200$	88.3	152.7	90.2	161.2
$t = 250, t^+ = 150$	88.7	120.8	89.8	124.8
$t = 300, t^+ = 100$	89.6	91.3	90.2	93.0
$t = 350, t^+ = 50$	89.8	60.5	90.1	60.9

Table 5: The mean (over repeated sampling) of the true coverage probability and width of an intended 90% prediction interval for N_{\bullet}^+ with $C = 20$ using the unadjusted and adjusted method.

	Unadjusted		Adjusted	
	Coverage (%)	w	Coverage (%)	w
$t = 50, t^+ = 350$	59.2	46.5	89.7	88.3
$t = 100, t^+ = 300$	73.4	40.2	89.9	58.0
$t = 150, t^+ = 250$	80.3	34.5	89.9	43.4
$t = 200, t^+ = 200$	84.1	29.1	90.0	33.7
$t = 250, t^+ = 150$	86.5	23.8	90.0	26.0
$t = 300, t^+ = 100$	87.8	18.4	89.8	19.4
$t = 350, t^+ = 50$	88.4	12.4	89.3	12.7

Table 6: The mean (over repeated sampling) of the true coverage probability and width of an intended 95% prediction interval for N_{\bullet}^+ using the unadjusted and adjusted method.

	Unadjusted		Adjusted	
	Coverage (%)	w	Coverage (%)	w
$t = 50, t^+ = 350$	72.0	167.4	94.4	292.7
$t = 100, t^+ = 300$	84.2	140.9	94.8	191.7
$t = 150, t^+ = 250$	88.9	118.0	94.7	143.0
$t = 200, t^+ = 200$	91.3	97.9	94.7	110.7
$t = 250, t^+ = 150$	92.8	79.4	94.8	85.8
$t = 300, t^+ = 100$	93.8	61.2	94.9	63.9
$t = 350, t^+ = 50$	94.5	41.1	94.9	41.9

Table 7: The mean (over repeated sampling) of the true coverage probability and width of an intended 90% prediction interval for T^+ with $n_{\bullet}^+ = 200$ using the unadjusted and adjusted method.

	Unadjusted		Adjusted	
	Coverage (%)	w	Coverage (%)	w
$t = 50$	73.9	28.7	89.6	41.5
$t = 100$	82.4	27.7	89.7	33.4
$t = 150$	85.4	27.0	89.7	30.4
$t = 200$	86.8	26.5	89.7	28.8
$t = 300$	88.2	25.9	89.8	27.1
$t = 500$	89.4	25.1	90.1	25.6
$t = 1000$	89.8	24.4	90.0	24.5

Table 8: The mean (over repeated sampling) true coverage probability and width of an intended 90% prediction interval for T^+ with $n_{\bullet}^+ = 200$ using the unadjusted and adjusted method for opening time Scenario 1.

	t^*	t^*/t_c	$n_{\bullet}^*/n_{\bullet}$	Unadjusted		Adjusted	
				Coverage (%)	w	Coverage (%)	w
$t = 50$	23.9	0.955	0.954	62.2	29.5	90.1	55.8
$t = 100$	46.1	0.920	0.919	73.6	28.7	90.1	42.6
$t = 150$	66.8	0.890	0.890	78.3	28.4	89.8	37.6
$t = 200$	86.6	0.865	0.865	81.2	27.9	89.8	34.7
$t = 300$	123.9	0.825	0.825	84.4	27.3	89.9	31.7
$t = 500$	192.6	0.770	0.769	86.8	26.6	89.9	29.0
$t = 1000$	344.7	0.689	0.688	88.3	25.7	89.6	26.6

Table 9: The mean (over repeated sampling) coverage and width of an intended 90% prediction interval for T^+ with $n_{\bullet}^+ = 200$ using the unadjusted and adjusted method for opening time Scenario 2.

				Unadjusted		Adjusted	
	t^*	t^*/t_c	$n_{\bullet}^*/n_{\bullet}$	Coverage (%)	w	Coverage (%)	w
$t = 50$	21.6	0.863	0.860	59.6	30.1	90.2	59.1
$t = 100$	38.0	0.761	0.758	70.7	29.3	90.3	46.2
$t = 150$	50.8	0.678	0.675	75.2	29.0	90.2	41.4
$t = 200$	61.1	0.611	0.608	77.6	28.7	90.0	38.9
$t = 300$	76.6	0.511	0.508	79.9	28.4	89.8	36.2
$t = 500$	96.4	0.386	0.384	82.6	28.0	90.1	33.9
$t = 1000$	120.1	0.240	0.239	83.7	27.6	89.5	32.1